



THE UNIVERSITY *of* EDINBURGH

Edinburgh Research Explorer

[Cr

III8

M

II6

]

n+

(M

II

= Cu, Co) face-centred, metallosupramolecular cubes

Citation for published version:

O'Connor, HM, Sanz, S, Pitak, MB, Coles, SJ, Nichol, GS, Piligkos, S, Lusby, PJ & Brechin, EK 2016, '[Cr

III8

M

II6

]

n+

(M

II

= Cu, Co) face-centred, metallosupramolecular cubes' CrystEngComm, vol. 18, no. 26, pp. 4914-4920. DOI: 10.1039/C6CE00654J, 10.1039/c6ce00654j

Digital Object Identifier (DOI):

[10.1039/C6CE00654J](https://doi.org/10.1039/C6CE00654J)

[10.1039/c6ce00654j](https://doi.org/10.1039/c6ce00654j)

Link:

[Link to publication record in Edinburgh Research Explorer](#)

Document Version:

Peer reviewed version

Published In:

CrystEngComm

General rights

Copyright for the publications made accessible via the Edinburgh Research Explorer is retained by the author(s) and / or other copyright owners and it is a condition of accessing these publications that users recognise and abide by the legal requirements associated with these rights.



[Cr^{III}₈M^{II}₆]ⁿ⁺ (M^{II} = Cu, Co) face-centred, metallosupramolecular cubes

Received 00th January 20xx,
Accepted 00th January 20xx

H. M. O'Connor,^{a†} S. Sanz,^{*a†} M. B. Pitak,^b S. J. Coles,^b G. S. Nichol,^a S. Piligkos,^c P. J. Lusby^{*a} and E. K. Brechin^{*a}

DOI: 10.1039/x0xx00000x

www.rsc.org/

Four [Cr^{III}₈M^{II}₆]ⁿ⁺ (M^{II} = Cu, Co) coordination cubes of formulae [Cr₈Co₆L₂₄Cl₁₂] (**1**), [Cr₈Co₆L₂₄(SCN)₁₂] (**2**), [Cr₈Cu₆L₂₄(H₂O)₁₂](SO₄)₆ (**3**), and [Cr₈Cu₆L₂₄Cl₁₂] (**4**) (where HL is 1-(4-pyridyl)butane-1,3-dione), were synthesised using the [Cr^{III}L₃] metalloligand in combination with a variety of M^{II} salts. The metallic skeleton of each cage describes a cube in which the [Cr^{III}L₃] moieties occupy the eight vertices and the M^{II} ions lie at the centre of the six faces. The axial coordination sites of the M^{II} cations are occupied by either H₂O molecules or Cl⁻/SCN⁻ anions originating from the M^{II} salt used in the synthesis, resulting in neutral **1**, **2** and **4** and the cage in **3** being a 12+ cation; the charge-balancing SO₄²⁻ anions accommodated both inside and outside the cube. Magnetic susceptibility and magnetisation measurements reveal weak exchange between nearest neighbour metal ions, mediated *via* the L⁻ ligands. The modular assembly of the cubes suggests that any combination of [M^{III}L₃] metalloligand and M^{II} salt will work, potentially resulting in an enormous family of supramolecular assemblies. The charge of the cubes is controlled by the nature of the ligand occupying the axial sites on the M^{II} ions, suggesting trivial ligand exchange may offer control over, amongst others, solubility, reactivity, post-synthetic modification and substrate specificity. The large internal cavities of the cubes also suggest host-guest chemistry may be a fruitful route to encapsulating magnetic and/or redox active guests which could be employed to control magnetic behaviour, and the construction of multifunctional materials.

Introduction

Metallosupramolecular chemistry relies on the use of dynamic metal-ligand bonds for the construction of multinuclear coordination assemblies.^{1,2} From a design perspective, the selection of a particular metal ion can have numerous implications on the outcome of any given assembly reaction because they provide differing coordination geometry preferences, and a range of binding strengths, which often show a strong correlation with substitutional lability.³ Given this potential variation in metal-ion component and the capacity to readily access multitopic ligands with differing coordination vectors, it is perhaps not surprising that this rational design approach has yielded a vast array of discrete nanostructures of varying shape, size and nuclearity.^{4,5} Often, the combination of highly directional metal-ligand bonding and the rigid nature of the ligand framework creates a molecular scaffold that defines the boundaries of a permanent internal cavity.^{2,4,5} These

discrete void areas impart unique properties to the structure allowing for numerous applications⁶ in areas such as gas adsorption,^{7,8} stabilisation of reactive molecules,⁹ catalysis,¹⁰ biochemical and biomedical applications,¹¹ separation of species from a mixture¹², and development of magnetic materials.^{8,13}

In the field of molecular magnetism the systematic exploration of ligand design, metal identity and reaction conditions is employed to build families of structurally related complexes whose subsequent physical characterisation reveals the underlying principles behind the magneto-structural relationship.¹⁴ Geometric and molecular symmetry, for example, defines a range of fascinating, and potentially useful low temperature physics, ranging from spin-frustrated molecules to anisotropic metal cages behaving like nanoscale magnets.^{15,16} Judicious ligand design is the first stage of the synthetic process,¹⁷ and the use of rigid ligands with fixed coordination modes allows for the construction of cages with predictable topologies,¹⁸ and potentially those that possess cavities capable of binding guest molecules. However, while the host-guest chemistry of diamagnetic coordination capsules has been widely studied and exploited, magnetic coordination capsules and the study of the interaction between magnetic hosts and guests has largely been ignored.^{8,19}

Recently we embarked on a new project that would enable heterometallic paramagnetic coordination cages to be accessed in a modular and predictable fashion,²⁰ an approach centred around the tritopic "metalloligand", [M^{III}L₃] (HL = 1-(4-

^aH. M. O'Connor, Dr S. Sanz, Dr G. S. Nichol, Dr P. J. Lusby, Prof. E. K. Brechin, EaStCHEM School of Chemistry, The University of Edinburgh, David Brewster Road, Edinburgh, EH9 3FJ, UK. E-mail: E.Brechin@ed.ac.uk; S.Calvo@ed.ac.uk; Paul.Lusby@ed.ac.uk

^bDr M. Pitak, Dr S. J. Coles, UK National Crystallography Service, Chemistry, University of Southampton, Southampton, Highfield Campus, SO17 1BJ, UK.

^cDr S. Piligkos, Department of Chemistry, University of Copenhagen, Universitetsparken 5, DK-2100, Copenhagen, Denmark.

[†]S. Sanz and H. M. O'Connor contributed equally to this work. Electronic Supplementary Information (ESI) available: [details of any supplementary information available should be included here]. See DOI: 10.1039/x0xx00000x

pyridyl)butane-1,3-dione), which features a tris(acac) octahedral transition metal core pendant functionalised with three *p*-pyridyl donor groups (Figure 1).

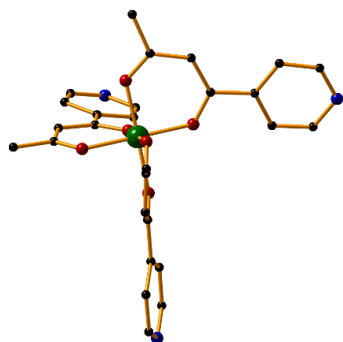


Figure 1. The molecular structure of $[\text{Cr}^{\text{III}}\text{L}_3]$. Colour code: Cr = green, O = red, N = blue, C = grey. H=atoms omitted.

In the case of the *fac*-isomer, the *N*-donor groups are aligned in a tripodal array such that the entropically-favoured smallest assembly that ensures maximum-site occupancy with a square-planar connector would be a cubic system.²⁰ As such, we would be able to use pre-designed self-assembly to position one metallic [and paramagnetic] ion at the eight cube vertices and another at the centre of the six faces. Herein, we report the preparation and structural data of four heterometallic $[\text{Cr}^{\text{III}}_8\text{M}^{\text{II}}_6]^{n+}$ molecular cubes, where $\text{M}^{\text{II}} = \text{Cu}, \text{Co}$, along with a discussion of their magnetic behaviour.

Experimental section

Syntheses

1-(4-pyridyl)butane-1,3-dione (HL) and the metalloligand $[\text{CrL}_3]$ were prepared according to previously published procedures.^{20,21} All reactions were performed under aerobic conditions. Solvents and reagents were used as received from commercial suppliers. Variable-temperature, solid-state direct current (dc) magnetic susceptibility and variable-temperature-and-variable-field (VTVB) magnetisation data down to $T = 2$ K were collected on a Quantum Design MPMS-XL SQUID magnetometer equipped with a 7 T dc magnet.

$[\text{Cr}_8\text{Co}_6\text{L}_{24}\text{Cl}_{12}]$ (**1**)

To a solution of the metalloligand $[\text{CrL}_3]$ (108 mg, 0.2 mmol) in 20 mL of dichloromethane/tetrahydrofuran (1:1 v/v) was added CoCl_2 (20 mg, 0.15 mmol). The solution was stirred for 14 hours, before being filtered and allowed to stand. Brown, X-ray quality crystals were obtained after room temperature evaporation of the mother liquor after 5 days. Elemental analysis (%) calculated (found): C 51.84 (51.61), H 4.20 (4.09), N 6.25 (6.54). Yield = 63%.

$[\text{Cr}_8\text{Co}_6\text{L}_{24}(\text{SCN})_{12}]$ (**2**)

To a solution of the metalloligand $[\text{CrL}_3]$ (108 mg, 0.2 mmol) in 20 mL of dichloromethane/methanol (1:1 v/v) was added $\text{Co}(\text{SCN})_2$ (35 mg, 0.2 mmol). The solution was stirred for 2 hours, before being filtered and allowed to stand. Brown, X-ray quality crystals were obtained after room temperature evaporation of the mother liquor after 5 days. Elemental

analysis (%) calculated (found): C 53.63 (53.26), H 3.79 (3.51), N 4.94 (5.13). Yield = 77%.

$[\text{Cr}_8\text{Cu}_6\text{L}_{24}(\text{H}_2\text{O})_{12}](\text{SO}_4)_6$ (**3**)

To a solution of the metalloligand $[\text{CrL}_3]$ (108 mg, 0.2 mmol) in 20 mL of dichloromethane/methanol (1:1 v/v) was added a solution of $\text{Cu}(\text{SO}_4)\cdot 5\text{H}_2\text{O}$ (50 mg, 0.2 mmol) in 3 mL of water. The solution was stirred for 1 hour, before being filtered and allowed to stand. Green X-ray quality crystals were obtained after room temperature evaporation of the mother liquor after 5 days. Elemental analysis (%) calculated (found): C 47.33 (47.12), H 3.97 (3.83), N 6.13 (5.97). Yield = 59%.

$[\text{Cr}_8\text{Cu}_6\text{L}_{24}\text{Cl}_{12}]$ (**4**)

To a solution of the metalloligand $[\text{CrL}_3]$ (108 mg, 0.2 mmol) in 20 mL of dichloromethane/methanol (1:1 v/v) was added a solution of $\text{CuCl}_2\cdot 2\text{H}_2\text{O}$ (34 mg, 0.2 mmol) in 2 mL of water. The solution was stirred for 5 minutes before being filtered and allowed to stand. Green-brown, X-ray quality crystals were obtained after room temperature evaporation of the mother liquor after 5 days. Elemental analysis (%) calculated (found): C 50.72 (50.43), H 3.78 (3.45), N 6.57 (6.64). Yield = 68%.

Crystal structure information

For compounds **1**, **2** and **4** single-crystal X-ray diffraction data were collected at $T = 100$ K on a Rigaku AFC12 goniometer equipped with an enhanced sensitivity (HG) Saturn 724+ detector mounted at the window of an FR-E+ Superbright MoK α rotating anode generator with HF Varimax optics (70 μm focus)²² using Rigaku Crystal Clear and CrysAlisPro software^{23,24} for data collection and reduction. For compound **3** and $[\text{Cr}^{\text{III}}\text{L}_3]$ single crystal X-ray diffraction data were measured on a Rigaku Oxford Diffraction SuperNova diffractometer using Mo (for $[\text{Cr}^{\text{III}}\text{L}_3]$) or Cu (for **3**) radiation at $T = 120$ K. The CrysAlisPro software package was used for instrument control, unit cell determination and data reduction.²⁵ Unit cell parameters in all cases were refined against all data. Crystal structures were solved using the charge flipping method implemented in SUPERFLIP²⁶ (**1**, **2**, and **4**), Olex2 ($[\text{Cr}^{\text{III}}\text{L}_3]$), or by direct methods with ShelXS (**3**). All structures were refined on F_o^2 by full-matrix least-squares refinements using ShelXL²⁷ within the OLEX2 suite.²⁸ All non-hydrogen atoms were refined with anisotropic displacement parameters, and all hydrogen atoms were added at calculated positions and refined using a riding model with isotropic displacement parameters based on the equivalent isotropic displacement parameter (U_{eq}) of the parent atom.

Crystal data for $[\text{Cr}^{\text{III}}\text{L}_3]$: $\text{C}_{27}\text{H}_{24}\text{N}_3\text{O}_6\text{Cr}$, $M_r = 538.49$, trigonal, $a = 17.6411(3)$ Å, $b = 17.6411(3)$ Å, $c = 27.0463(4)$ Å, $\alpha = 90.0^\circ$, $\beta = 90.0^\circ$, $\gamma = 120.0^\circ$, $V = 7289.3(2)$ Å³, $Z = 12$, $R-3$, $D_c = 1.472$ g/cm³, $\mu = 0.520$ mm⁻¹, $T = 120$ K, 5148 unique reflections ($R_{\text{int}} = 0.0473$), 4803 with $F^2 > 2\sigma$, $R(F, F^2 > 2\sigma) = 0.0561$, $R_w(F^2, \text{all data}) = 0.1096$.

*Crystal data for **1**:* $\text{C}_{232}\text{H}_{224}\text{N}_{24}\text{O}_{52}\text{Cl}_{12}\text{Cr}_8\text{Co}_6$, $M_r = 5375.43$, triclinic, $a = 28.265(4)$ Å, $b = 29.830(4)$ Å, $c = 31.290(5)$ Å, $\alpha = 72.023(16)^\circ$, $\beta = 71.093(15)^\circ$, $\gamma = 63.981(13)^\circ$, $V = 21995(7)$ Å³, $Z = 2$, $P-1$, $D_c = 0.812$ g/cm³, $\mu = 0.526$ mm⁻¹, $T = 100(2)$ K, 73957 unique reflections ($R_{\text{int}} = 0.0635$), 49534 with $F^2 > 2\sigma$, $R(F, F^2 > 2\sigma) = 0.1299$, $R_w(F^2, \text{all data}) = 0.4175$.

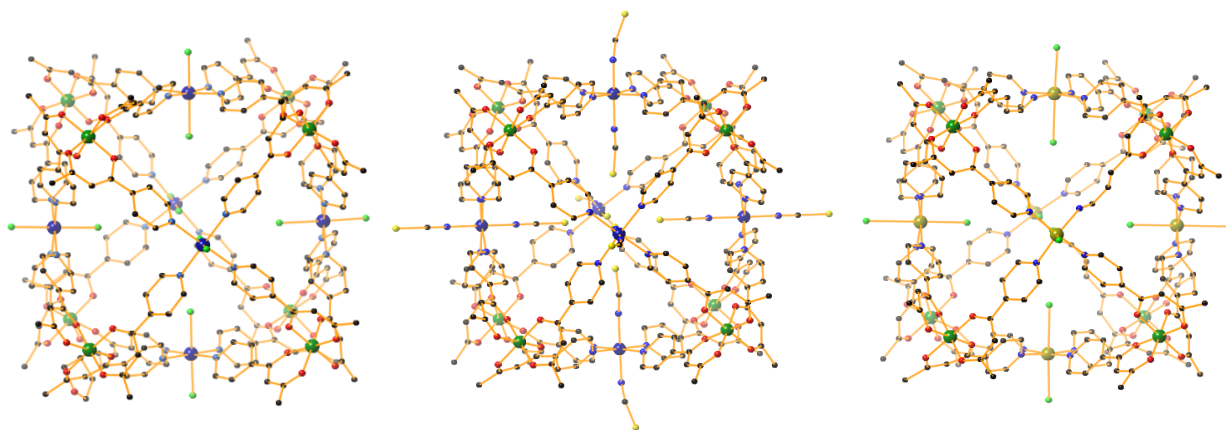


Figure 2. From left to right, molecular structures of **1**, **2** and **4**. Colour code: Cr = green, Co = blue, Cu = olive, O = red, N = blue, S = yellow, Cl = light-green, C = black. H-atoms omitted for clarity.

Crystal data for 2: $C_{228}H_{192}N_{36}O_{48}S_{12}Cr_8Co_6$, $M_r = 5106.41$, tetragonal, $a = 41.7282(5) \text{ \AA}$, $b = 41.7282(5) \text{ \AA}$, $c = 30.6665(7) \text{ \AA}$, $\alpha = \beta = \gamma = 90.0^\circ$, $V = 53397.9(18) \text{ \AA}^3$, $Z = 4$, $I4_122$, $D_c = 0.667 \text{ g/cm}^3$, $\mu = 0.420 \text{ mm}^{-1}$, $T = 100(2) \text{ K}$, 23556 unique reflections ($R_{int} = 0.1250$), 10357 with $F^2 > 2\sigma$, $R(F, F^2 > 2\sigma) = 0.0457$, $R_w(F^2, \text{all data}) = 0.0941$.

Crystal data for 3: $C_{216}H_{216}N_{24}O_{48}S_6Cr_8Cu_6$, $M_r = 5481.79$, tetragonal, $a = 28.79166(19) \text{ \AA}$, $b = 28.79166(19) \text{ \AA}$, $c = 24.4854(3) \text{ \AA}$, $\alpha = \beta = \gamma = 90.0^\circ$, $V = 20297.4(4) \text{ \AA}^3$, $Z = 2$, $P4/n$, $D_c = 0.897 \text{ g/cm}^3$, $\mu = 2.782 \text{ mm}^{-1}$, $T = 120 \text{ K}$, 16958 unique reflections ($R_{int} = 0.0762$), 11352 with $F^2 > 2\sigma$, $R(F, F^2 > 2\sigma) = 0.1208$, $R_w(F^2, \text{all data}) = 0.3932$.

Crystal data for 4: $C_{216}H_{192}N_{24}O_{48}Cl_{12}Cr_8Cu_6$, $M_r = 5114.68$, tetragonal, $a = 41.329(14) \text{ \AA}$, $b = 41.329(14) \text{ \AA}$, $c = 31.056(10) \text{ \AA}$, $\alpha = \beta = \gamma = 90.0^\circ$, $V = 53046(40) \text{ \AA}^3$, $Z = 4$, $I4_122$, $D_c = 0.640 \text{ g/cm}^3$, $\mu = 0.486 \text{ mm}^{-1}$, $T = 100(2) \text{ K}$, 23152 unique reflections ($R_{int} = 0.1250$), 11046 with $F^2 > 2\sigma$, $R(F, F^2 > 2\sigma) = 0.0424$, $R_w(F^2, \text{all data}) = 0.1118$.

CCDC 1457376-1457380.

Crystallography discussion

Crystals of all samples were very sensitive to solvent loss, which resulted in rapid crystal delamination and poor quality X-ray diffraction data. To slow down this crystal degradation, crystals of compounds **1**, **2** and **4** were 'cold mounted' on MiTeGen Micromounts™ at $T = 203 \text{ K}$ using Sigma-Aldrich Fomblin Y® LVAC (3300 mol. wt.) with the X-Temp 2²⁹ crystal cooling system attached to the microscope. This procedure protected crystal quality and permitted collection of usable X-ray data. All four structures contain large accessible voids and channels that are filled with diffuse electron density belonging to uncoordinated solvent, whose electron contribution was accounted for by the SMTBX solvent masking routine as implemented in OLEX2 software. The crystal structure of **1** exhibits a significant amount of positional disorder, whereby part of the complex adopts two positions along the Cl3-Co2-Cl4 axis. This disorder has been modelled over two sites with a 60:40 ratio. Several geometrical constraints (DFIX, AFIX 66, FLAT) have been used to maintain sensible molecular geometry.

Crystal structures **2** and **4** (both in the tetragonal $I4_122$ space group) have been refined as two-component inversion twins with 81:19 and 58:42 ratios, respectively. Global SIMU, RIGU and DELU restraints were used to model atomic displacement parameters. For structure **3**, the measured data were consistently of poor quality. This structure has been modelled as far as is reasonable and practical, given the poor quality of the data set. The ShelX weighting scheme could not be optimized. The Cu_6Cr_8 cage was identified easily from the initial structure solution and refines well without restraints. Overall the cube carries a total charge of 12+. This is balanced by six sulphate anions. Peaks in the difference map corresponding to three crystallographically inequivalent sulphate anions per asymmetric unit were identified. Of these, two are inside the cube (S2 and S3) and one (S1) is outside of the cube. The geometry of the S1 anion is the most stable, and thus S2 and S3 anions were modelled to have similar geometries to S1. S1 and S2 were refined anisotropically with displacement ellipsoid restraints; S3 was refined using an isotropic model. Each sulphate anion was modelled as half-occupied, and each is disordered around a crystallographic four-fold rotation axis so that the charges balance. Bond distance and displacement similarity restraints (SADI and RIGU) were used, as shown in the .res file embedded within the CIF shelx_res_file. Close O...O contacts between sulphate anions are flagged by PLATON; this is inevitable given the disordered nature of the anions. The copper centres are assumed to have axial aqua ligands, with the H atoms on these ligands placed for the sake of chemical completeness. The SQUEEZE routine of PLATON³⁰ was used to remove the remaining electron density, corresponding to 2934 electrons per unit cell. It is not good practice to attempt to ascribe this much electron density to either of the two solvents employed, methanol and dichloromethane, or to adventitious water molecules, as the ratio of solvents cannot be established by any other means. There is one residual peak of approximately 6.6 electrons located in the centre of the cube. There is no chemically plausible model for this, given the reagents and solvents used.

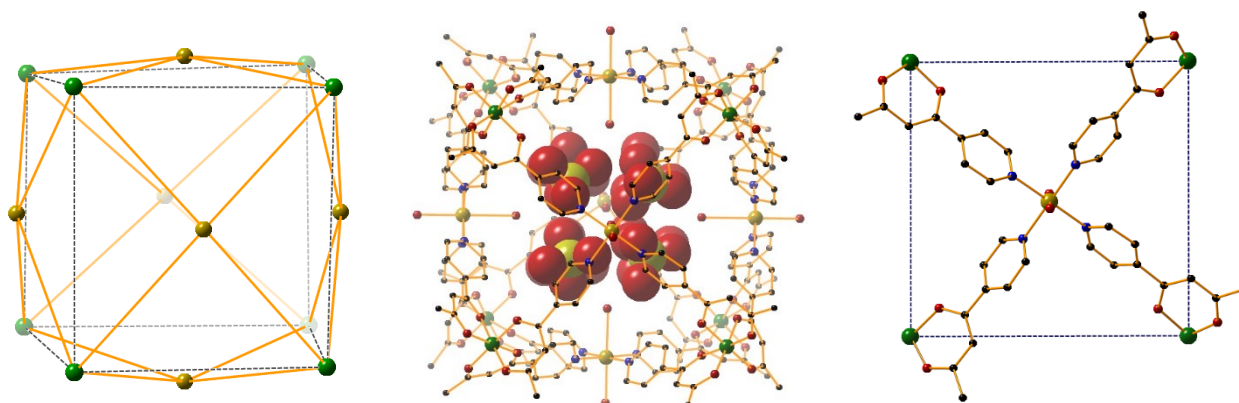


Figure 3. Metallic skeleton of the cation of complex **3** (left). The distance between nearest neighbour Cr^{III} and Cu^{II} ions is approximately 8.8 Å. The molecular structure of **3** (centre) highlighting the encapsulation of four SO₄²⁻ molecules in the internal cavity of the cage. H-atoms and external SO₄²⁻ anions have been omitted for clarity. Representation of one of the six faces of the cube (right), highlighting the coordination geometry of the Cu^{II} ion. The Cu^{II} ion is six coordinate with a {CuN₄O₂} coordination sphere; the Jahn-Teller distortion lying along the O-Cu-O vector, perpendicular to the face of the cube. Colour code: Cr = green, Cu = gold, O = red, N = blue, C = black.

Results and discussion

The heterometallic cages [Cr^{III}₈Co^{II}₆L₂₄Cl₁₂] (**1**), [Cr^{III}₈Co^{II}₆L₂₄(SCN)₁₂] (**2**), [Cr^{III}₈Cu^{II}₆L₂₄(H₂O)₁₂](SO₄)₆ (**3**) and [Cr^{III}₈Cu^{II}₆L₂₄Cl₁₂] (**4**) were all prepared in a similar manner by addition of an M^{II} salt to the metalloligand [Cr^{III}L₃] (HL = 1-(4-pyridyl)butane-1,3-dione) in a mixed solvent system (either CH₂Cl₂ / MeOH or CH₂Cl₂ / THF, see the experimental section for full details). The resultant reactions were stirred for a period of 1-14 hours, before being filtered; crystals were obtained by slow evaporation of the mother liquor at room temperature over several days. All four structures (Figures 2-3) reveal a similar pseudo-cubic metallic skeleton [Cr^{III}₈M^{II}₆]¹²⁺ where each M^{II} (M^{II} = Co, Cu) ion is situated slightly above (1.2-1.4 Å) the centre of a square face of approximate dimensions 12 Å, defined by four Cr ions. Each [Cr^{III}L₃] corner unit consists of a six-coordinate Cr ion with regular {CrO₆} octahedral geometry, with Cr-O distances between 1.86-2.01 Å and *cis/trans* angles in the range 85.6-94.2° and 176.3-179.5°, respectively. The face-centred linkage of each corner fragment is achieved by the coordination of the four pyridyl donors to the equatorial positions of the six-coordinate M^{II} metal ions, with M^{II}-N distances in the range 2-2.2 Å. For **1**, **2** and **4**, the remaining apical sites of each M^{II} ion are occupied by the anions present in the starting cobalt or copper salts (*i.e.* Cl⁻ or SCN⁻) giving overall charge neutral cages. However, with **3**, the apical sites are occupied by water molecules (arising from either the hydrated metal salt or from the non-dried solvent), which gives an assembly with overall +12 charge. Charge balance is maintained through the presence of a total of six SO₄²⁻ anions, four inside and two outside the cube (Figure 3). The Jahn-Teller axis of each Cu^{II} ion in **3** and **4** lies perpendicular to the face it sits in.

All four structures reveal that **1-4** crystallise as homochiral racemates, *i.e.* each cube possesses eight [Cr^{III}L₃] stereocentres of the same Λ or Δ chirality. While it is possible that this could simply be a packing effect from a complex and dynamic diastereomeric mixture, solution-based self-sorting of

assemblies that contain multimetallic stereocenters is a common,³¹ if not universal,³² occurrence. The energetic preference for a single diastereomer is a sign that stereochemical information between adjacent metal vertices is efficiently transmitted through the ligand framework. In the case of **1-4**, the [Cr^{III}L₃] stereocentres communicate *via* the tetrapyrridyl-M^{II} coordination motif, which exhibit pronounced propeller-like twists (rather than idealised D_{4h} symmetry). Interestingly, the sense of this twist is conserved over the six connected faces of each individual assembly; the opposite holds for connecting [Cr^{III}L₃] fragments of alternate stereochemistry.

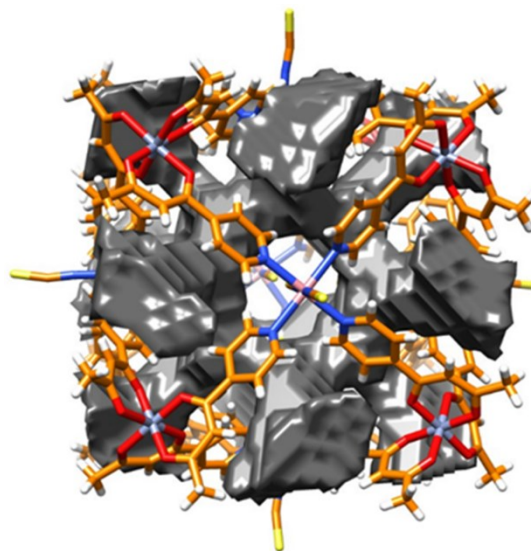


Figure 4. Representation of the available internal cavity space in complex **2**. A volume of 1471 Å³ was calculated employing an outer probe of 8.0 Å and an internal probe of 1.5 Å. See reference 33 for details.

Cr...Cr distances between nearest neighbours along the edges of the cubes measure approximately 12 Å, creating an internal volume of ~1400 Å³ per cage. Volume calculations performed on all four complexes with the ³V Volume Assessor programme,³³ which operates by rolling a virtual probe on the surface of a macromolecule, confirm this. A representation of the available internal cavity space in **2** is shown in Figure 4 as an example. The binding of molecules of suitable dimensions in the internal cavity of a molecular receptor in solution can be expected when the packing coefficient, that is, the ratio of the guest volume to the host volume, is approximately 0.55.³⁴ This suggests that guests with a total volume of ~770 Å³ could be

accommodated in compounds **1-4**. Indeed this is in accordance with the encapsulation of four SO_4^{2-} anions, with total volume of 668 \AA^3 , inside the cavity of complex **3** (Figure 3). Future work will focus on examining the host-guest chemistry of these cages, since their large internal cavities could potentially play host to an array of different species. For example, one can imagine constructing magnetic coordination capsules capable of hosting magnetic and/or redox-active guests, exerting control over magnetic super-exchange between metal ions in the host framework and between the host and guest.

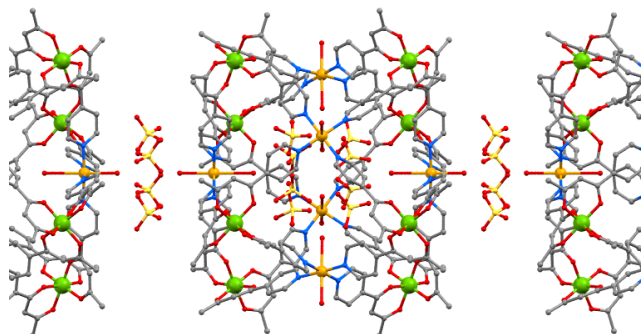


Figure 5. The packing of three molecules of compound **3** in the crystal, highlighting the H-bonded chains of cubes along the *c*-axis of the cell.

There are several close intermolecular contacts between the cages in the extended structures of **1-4**. In **1** the closest intercluster contacts are between the halide ions on one cube and the L⁻ ligands of the neighbouring cage with $\text{Cl}\cdots\text{C}$ distances in the range $3.6\text{-}3.9 \text{ \AA}$, while for **2** the closest contact is between the O- and C-atoms of the L⁻ ligands, with distances as short as 3.3 \AA . Similar ligand-ligand interactions also occur between the corners of the cubes in **3** and **4**, but in addition the externally located SO_4^{2-} ions in **3** H-bond to the terminally bonded H_2O molecules on the M^{II} ions ($\text{O}\cdots\text{O}$, 2.7 \AA), directing the formation of chains of clusters along the *c*-axis of the cell (Figure 5).

Magnetic studies

Quantitatively analysing the magnetic behaviour of such large heterometallic species using traditional matrix diagonalisation techniques is non-trivial, and often impossible, due to the enormous dimensions of the associated spin-Hamiltonian matrices. For complexes **1** and **2** analysis is further hindered by the presence of the highly anisotropic octahedral Co^{II} ion. As such we do not attempt fits of the susceptibility and magnetisation data, but instead simply compare the experimental data to the detailed magnetothermal and spectroscopic investigation of the structurally similar complexes $[\text{Cr}^{\text{III}}_8\text{Co}^{\text{II}}_6\text{L}_{24}(\text{H}_2\text{O})_{12}](\text{ClO}_4)_{12}$ (**5**) and $[\text{Cr}^{\text{III}}_8\text{Cu}^{\text{II}}_6\text{L}_{24}(\text{H}_2\text{O})_{10}(\text{NO}_3)_2](\text{NO}_3)_{10}$ (**6**) reported in reference 20, in which computational techniques known in theoretical nuclear physics as statistical spectroscopy were employed. The dc (direct current) molar magnetic susceptibility, χ_M , of polycrystalline samples of complexes **1-4** were measured in an applied magnetic field, *B*, of 0.1 T , over the $T = 5\text{-}300 \text{ K}$ temperature range (Figure 6); where $\chi_M = M/B$, and *M* is the magnetisation. At room temperature, the $\chi_M T$ products of **1 - 2**

and **3 - 4** have values of 26.3 and $17.7 \text{ cm}^3 \text{ mol}^{-1} \text{ K}$, respectively, in excellent agreement with that expected from the spin-only contributions to the magnetism of a $[\text{Cr}^{\text{III}}_8\text{Co}^{\text{II}}_6]$ unit ($26.3 \text{ cm}^3 \text{ mol}^{-1} \text{ K}$) with $g_{\text{Cr}} = g_{\text{Co}} = 2.00$, and of a $[\text{Cr}^{\text{III}}_8\text{Cu}^{\text{II}}_6]$ unit ($17.6 \text{ cm}^3 \text{ mol}^{-1} \text{ K}$), with $g_{\text{Cr}} = 2.00$ and $g_{\text{Cu}} = 2.15$, where g_{Cr} , g_{Co} , and g_{Cu} are the *g*-factors of Cr^{III} , Co^{II} and Cu^{II} , respectively. Upon cooling, the $\chi_M T$ values of **1-2** decrease continuously reaching a low temperature value of $\sim 20 \text{ cm}^3 \text{ mol}^{-1} \text{ K}$. The behaviour of complexes **3-4** appears, at least upon initial inspection, to be somewhat different. Upon cooling, the $\chi_M T$ products of both remain essentially constant down to $T = 20 \text{ K}$, below which there is an increase to a value of $\sim 18.5 \text{ cm}^3 \text{ mol}^{-1} \text{ K}$. Qualitatively the magnetic behaviour of **3** and **4** is straightforward: the exchange between the Cr^{III} and Cu^{II} ions is very weak and ferromagnetic in nature. One can also come to the same conclusion for compounds **1** and **2** [and **5**] if one assumes the high temperature decrease in $\chi_M T$ is due solely to the anisotropy of the octahedral Co^{II} ion. Indeed, the data for **5** shows a low temperature increase in $\chi_M T$ which is consistent with a weakly ferromagnetic $\text{Cr}^{\text{III}}\text{-Co}^{\text{II}}$ interaction. Clearly, however, other models invoking an antiferromagnetic interaction could explain the variable temperature susceptibility.²⁰ Variable-temperature-and-variable-field (VTVB) magnetisation studies are consistent with the presence of weak exchange interactions in all cases (Figure 6, bottom), with the saturation magnetic moment at $T = 2 \text{ K}$ and $B = 7 \text{ T}$ being close to that expected for a fully parallel alignment of the spins in the case of the Cr-Cu cages. For the Cr-Co cages **1** and **2** the saturation magnetic moments are lower than the ferromagnetic limit due to the large orbital contribution of the octahedral Co^{II} ion.^{20a}

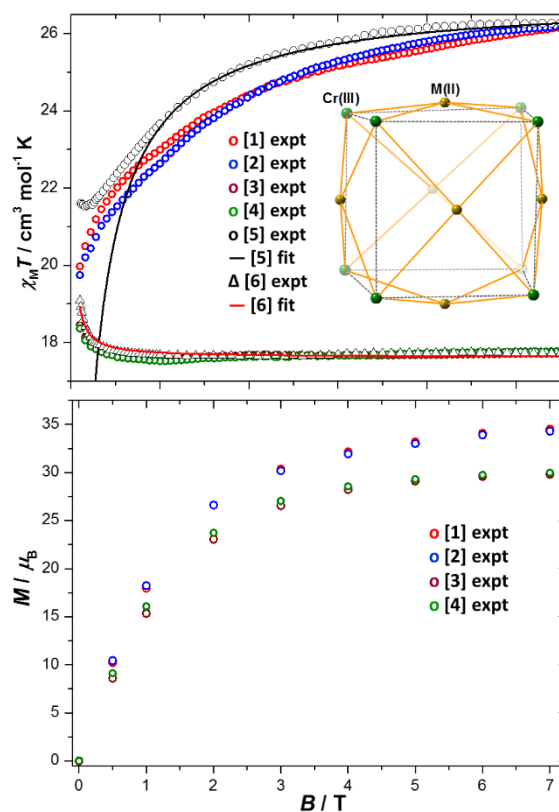


Figure 6. Plot of the $\chi_M T$ product versus temperature for complexes **1-4** (top). The data for complexes **5** and **6** are added for comparison. See reference 20 for full

details of the fits for **5** and **6**. Plot of the VTVB magnetisation data for complexes **1-4** (bottom).

Conclusions

The modular assembly of magnetic coordination capsules with internal cavities capable of hosting magnetic and redox-active guests is an under-explored field of research that can be exploited for the construction of tuneable, multifunctional molecular magnets with potential application in information storage and molecular spintronics. The ability to control and manipulate (switch on, switch off) magnetic exchange between metal ions in the host framework and between the host and guest(s) *via* the use of redox-active (radical) ligands in the framework of the host, and/or redox-active/paramagnetic guests held within the cavities, remains an attractive target. The construction of said capsules in a manner amenable to exohedral functionalization such that the organic sheath surrounding the capsules are easily derivatised post-synthetically to modify and tune solubility, magnetic behaviour, reactivity, stability and substrate specificity would also make the cages suitable for materials applications.

Here, the simple, modular assembly of $[M^{III}_8M^{II}_6]^{n+}$ cubes [with $M^{III} = Cr$ and $M^{II} = Co, Cu$] suggests that any combination of $[M^{III}_8L_3]$ metalloligand and M^{II} salt will work, potentially resulting in an enormous family of supramolecular assemblies. The charge of the cubes varies from neutral to 12+ and is controlled by the nature of the ligand occupying the axial sites on the M^{II} ions. Ligand substitution at these sites should be trivial and may prove a gateway to accessing a variety of new cages and polymers whereby the clusters are linked *via* di/polytopic linker ligands. Complex **3** encapsulates four SO_4^{2-} ions in its central cavity (of volume $\sim 1400 \text{ \AA}^3$) suggesting that cationic cages may be good hosts for different guests, such as organic radicals or simple coordination compounds containing paramagnetic metal ions.

Heterometallic $Cr^{III}-Co^{II}$ cages are surprisingly rare. Excluding organometallic and metal-metal bonded species, a search of the Cambridge Structural Database returned just a handful of hits, and the vast majority of these are derivatives of the well-known $[Cr_7Co]$ wheels of Winpenny and Timco.³⁵ There are two hydroxo/alkoxo-bridge dimers,³⁶ linear trimers and the ubiquitous triangular basic carboxylates,³⁷ a Cr_2Co_2 butterfly and a Cr_3Co star,³⁸ and pivalate/phosphonate-bridged Cr_2Co_4 , Cr_4Co_8 and Cr_4Co_4 cages.³⁹ Heterometallic $Cr^{III}-Cu^{II}$ complexes are similarly dominated by Manchester wheels, but here there is a little more variety with Cr_7Cu , Cr_8Cu_2 , $Cr_{10}Cu_2$ and $Cr_{12}Cu_2$ examples all being reported.⁴⁰ Beyond these there is very little else in the literature, bar a few examples of dimers, Cr_2Cu trimers, Cr_2Cu_2 butterflies and one example of a Cr_2Cu_4 cage.⁴¹ The Cr_8Co_6 and Cr_8Cu_6 cages reported herein are therefore the largest such species yet reported.

Acknowledgements

EKB thanks the EPSRC for funding. MP and SJC thank the EPSRC for funding the UK National Crystallography service.

Notes and references

Crystallographic data (including structure factors) for **1-4** have been deposited with the Cambridge Crystallographic Data Centre. CCDC 1457376-1457380). Copies of the data can be obtained, free of charge, on application to Cambridge Crystallographic Data Centre, 12 Union Road, Cambridge CB2 1EZ, UK, (fax: +44-(0)1223-336033 or e-mail: deposit@ccdc.cam.ac.uk). Magnetic data has been deposited at Edinburgh Datashare: <http://datashare.is.ed.ac.uk/>

- See for example a) J.-M. Lehn, *Supramolecular Chemistry Concepts and Perspectives*, VCH, Weinheim, 1995; b) J. L. Atwood, J. E. D. Davies, J.-M. Lehn, D. D. MacNicol and F. Vogtle, *Comprehensive Supramolecular Chemistry*, Pergamon, Oxford, 1996.
- B. H. Northrop, Y.-R. Zheng, K.-W. Chi and P. J. Stang, *Acc. Chem. Res.*, 2009, **42**, 1554.
- J. Ribas, *Coordination Chemistry*, Wiley-VCH, 2008.
- T. R. Cook, Y. Zheng and P. J. Stang, *Chem. Rev.*, 2013, **113**, 734.
- R. Chakrabarty, P. S. Mukherjee and P. J. Stang, *Chem. Rev.*, 2011, **111**, 6810.
- M. Yoshizawa, J. K. Klosterman and M. Fujita, *Angew. Chem. Int. Ed.*, 2009, **48**, 3418.
- I. A. Riddell, M. M. J. Smulders, J. K. Clegg and J. R. Nitschke, *Chem. Commun.*, 2011, **47**, 457.
- M. B. Duriska, S. M. Neville, J. Lu, S. S. Iremonger, J. F. Boas, C. J. Kepert and S. R. Batten, *Angew. Chem. Int. Ed.*, 2009, **48**, 8919.
- See for example a) P. Mal, B. Breiner, K. Rissanen and J. R. Nitschke, *Science*, 2009, **324**, 1697; b) M. M. J. Smulders and J. R. Nitschke, *Chem. Sci.*, 2012, **3**, 785.
- See for example a) M. Yoshizawa, M. Tamura and M. Fujita, *Science*, 2006, **312**, 251; b) T. Murase, S. Horiuchi and M. Fujita, *J. Am. Chem. Soc.*, 2010, **132**, 2866; c) S. Horiuchi, Y. Nishioka, T. Murase and M. Fujita, *Chem. Commun.*, 2010, **46**, 3460.
- M. Hannon, *Chem. Soc. Rev.*, 2007, **36**, 280.
- a) Y. R. Hristova, M. M. J. Smulders, J. K. Clegg, B. Breiner and J. R. Nitschke, *Chem. Sci.*, 2011, **2**, 638; b) S. Turega, M. Whitehead, B. R. Hall, M. F. Haddow, C. A. Hunter and M. D. Ward, *Chem. Commun.*, 2012, **48**, 2752.
- E. Coronado and G. M. Espallargas, *Chem. Soc. Rev.*, 2013, **42**, 1525
- D. Gatteschi, O. Kahn and R. D. Willet, ed. *Magneto-Structural Correlations in Exchange-Coupled Systems*, D. Reidel: Dordrecht, 1985.
- J. Schnack, *Dalton Trans.*, 2010, **39**, 4677
- D. Gatteschi, R. Sessoli and J. Villain, *Molecular Nanomagnets*, Oxford University Press, Oxford, 2006.
- C. J. Milios and R. E. P. Winpenny, *Struct. Bond.*, 2015, **164**, 1.
- J. N. Rebilly and T. Mallah, *Struct. Bond.*, 2006, **122**, 103.
- a) J. J. Sokol, M. P. Shores and J. R. Long, *Angew. Chem. Int. Ed.*, 2001, **40**, 236; b) S. Wang, J. L. Zuo, H. C. Zhuo, H. J. Choi, Y. Ke, J. R. Long and X. Z. You, *Angew. Chem. Int. Ed.*, 2004, **43**, 5940; c) H. Kumari, C. L. Dennis, A. V. Mossine, C. A. Deakynne and J. L. Atwood, *J. Am. Chem. Soc.*, 2013, **135**, 7110. There are several metal-organic polyhedra based on paramagnetic metal ions, but in the main these have not targeted/reported magnetic behaviour. See for example: d) A. J. McConnell, C. S. Wood, P. P. Neelakandan and J. R. Nitschke, *Chem. Rev.*, 2015, **115**, 7729; e) C. J. Brown, F. D. Toste, R. G. Bergman and K. N. Raymond, *Chem. Rev.*, 2015, **115**, 3012; f) T. D. Hamilton, G. S. Papaefstathiou, T. Friščić, D.-K. Bucar and L. R. MacGillivray, *J. Am. Chem. Soc.*, 2008, **130**, 14366; g) H. Kumari, P. Jin, S. J. Teat, C. L. Barnes, S. J. Dalgarno and J. L. Atwood, *J. Am. Chem. Soc.*, 2014, **136**, 17002.

- 20 a) S. Sanz, H. M. O'Connor, E. M. Pineda, K. S. Pedersen, G. S. Nichol, O. Mønsted, H. Weihe, S. Piligkos, E. J. L. McInnes, P. J. Lusby and E. K. Brechin, *Angew. Chem. Int. Ed.*, 2015, **54**, 6761; b) an analogous, diamagnetic cage also exists: H.-B. Wu, Q.-M. Wang, *Angew. Chem. Int. Ed.*, 2009, **48**, 7343.
- 21 B. Singh, G. Y. Leshar, K. C. Pluncket, E. D. Pagani, D. C. Bode, R. G. Bentley, M. J. Connell, L. T. Hamel and P. J. Silver, *J. Med. Chem.*, 1992, **35**, 4858.
- 22 S. J. Coles and P. A. Gale, *Chem. Sci.*, 2012, **3**, 683.
- 23 CrystalClear-SM Expert 3.1 b27 (Rigaku, 2012).
- 24 CrysAlisPro 1.171.38.41 (Rigaku Oxford Diffraction, 2015).
- 25 CrysAlisPro, 2016, Rigaku Oxford Diffraction, Oxford, UK.
- 26 L. Palatinus and G. Chapuis, *J. Appl. Cryst.*, 2007, **40**, 786.
- 27 G. M. Sheldrick, *Acta Cryst.*, 2015, **71**, 3.
- 28 O. V. Dolomanov, A. J. Blake, N. R. Champness and M. Schröder, *J. Appl. Crystallogr.*, 2003, **36**, 1283.
- 29 T. Kottke and D. Stalke, *J. Appl. Crystallogr.*, 1993, **26**, 615.
- 30 A. L. Spek, *Acta Crystallogr. Sect. C.*, 2015, **71**, 9.
- 31 A. M. Castilla, W. J. Ramsay and J. R. Nitschke, *Acc. Chem. Res.* 2014, **47**, 2063.
- 32 O. Chepelin, J. Ujma, X. Wu, A. M. Z. Slawin, M. B. Pitak, S. J. Coles, J. Michel, A. C. Jones, P. E. Barran and P. J. Lusby, *J. Am. Chem. Soc.*, 2012, **134**, 19334.
- 33 N. R. Voss and M. Gerstein, *Nucleic Acids Res.*, 2010, **38**, W555.
- 34 S. Mecozzi and J. Rebek, *Chem. Eur. J.*, 1998, **4**, 1016.
- 35 E. C. Sañudo, T. B. Faust, C. A. Muryn, R. G. Pritchard, G. A. Timco and R. E. P. Winpenny, *Inorg. Chem.*, 2009, **48**, 9811.
- 36 a) P. Chaudhuri, M. Winter, J. Kueppers, K. Wiegardt, B. Nuber and J. Weiss, *Inorg. Chem.*, 1987, **26**, 3302; b) P. Alborès, J. Seeman and E. Rentschler, *Dalton Trans.*, 2009, 7660.
- 37 K. M. Corbin, D. J. Hodgson, M. H. Lynn, K. Michelsen, K. M. Nielsen and E. Pedersen, *Inorg. Chim. Acta*, 1989, **159**, 129.
- 38 a) V. V. Semenaka, O. V. Nesterova, V. N. Kokozay, R. I. Zibatyuk, O. V. Shishkin, R. Boca, C. J. Gómez-García, J. M. Clemente-Juan and J. Jezierska, *Polyhedron*, 2010, **29**, 1326; b) D. J. Hodgson, K. Michelsen, E. D. Towle, *J. Chem. Soc., Chem. Commun.*, 1988, 426.
- 39 Y.-Z. Zheng, B. A. Breeze, G. A. Timco, F. Tuna and R. E. P. Winpenny, *Dalton Trans.*, 2010, **39**, 6175.
- 40 a) B. Ballesteros, T. B. Faust, C.-F. Lee, D. A. Leigh, C. A. Muryn, R. G. Pritchard, D. Schultz, S. J. Teat, G. A. Timco and R. E. P. Winpenny, *J. Am. Chem. Soc.*, 2010, **132**, 15435; b) L. P. Engelhardt, C. A. Muryn, R. G. Pritchard, G. A. Timco, F. Tuna and R. E. P. Winpenny, *Angew. Chem. Int. Ed.*, 2008, **47**, 924; c) F. K. Larsen, J. Overgaard, S. Parsons, E. Rentschler, A. A. Smith, G. A. Timco and R. E. P. Winpenny, *Angew. Chem. Int. Ed.*, 2003, **42**, 5978; d) C.-F. Lee, D. A. Leigh, R. G. Pritchard, D. Schultz, S. J. Teat, G. A. Timco and R. E. P. Winpenny, *Nature*, 2009, **458**, 314; e) L. P. Engelhardt, C. A. Muryn, R. G. Pritchard, G. A. Timco, F. Tuna and R. E. P. Winpenny, *Angew. Chem. Int. Ed.*, 2008, **47**, 924.
- 41 See for example: a) J. A. Rusanova, V. V. Semenaka, V. V. Dyakonenko and O. V. Shishkin, *Acta Crystallogr., Sect. E: Cryst. Commun.*, 2015, **71**, 1077; b) G. Lorusso, V. Corradini, A. Candini, A. Ghirri, R. Biagi, U. d. Pennino, S. Carretta, E. Garlatti, P. Santini, G. Amoretti, G. Timco, R. G. Pritchard, R. E. P. Winpenny and M. Affronte, *Phys. Rev. B*, 2010, **82**, 144420; c) J. Glerup, P. A. Goodson, D. J. Hodgson, M. H. Lynn and K. Michelsen, *Inorg. Chem.*, 1992, **31**, 4785; d) S. Khanra, T. Weyhermuller and P. Chaudhuri, *Dalton Trans.*, 2007, 4675; e) F. S. Delgado, J. Sanchiz, T. Lopez, F. Lloret, M. Julve and C. Ruiz-Perez, *CrystEngComm.*, 2010, **12**, 2711.